International Journal of Nanomedicine Dovepress

Open Access Full Text Article ORIGINAL RESEARCH

Insight into Antiviral Activity of Ag/TiO_2 Nanocomposites Against Influenza H1N1 Virus and Its Antiviral Mechanism

Yihe Ma[1–3,*], Xiaojun Xiao[2,*], Yutao Wang[3,*], Jie Sun[4], Ping Tang[5], Jing Li[3], Xizhuo Sun[5], Damo Xu[1,2], Zifeng Yang[3], Shiguo Chen[4], Xiaoyu Liu[2]

[1]Department of Respiratory and Allergy, Third Affiliated Hospital of Shenzhen University, Shenzhen, People's Republic of China; [2]State Key Laboratory of Respiratory Disease for Allergy at Shenzhen University, Shenzhen Key Laboratory of Allergy & Immunology, School of Medicine, Shenzhen University, Shenzhen, People's Republic of China; [3]State Key Laboratory of Respiratory Disease, National Clinical Research Center for Respiratory Disease, Guangzhou Institute of Respiratory Health, the First Affiliated Hospital of Guangzhou Medical University, Guangzhou, People's Republic of China; [4]Nanshan District Key Laboratory for Biopolymers and Safety Evaluation, Shenzhen Key Laboratory of Polymer Science and Technology, Guangdong Research Center for Interfacial Engineering of Functional Materials, College of Materials Science and Engineering, Shenzhen University, Shenzhen, People's Republic of China; [5]Department of General Practice, Third Affiliated Hospital of Shenzhen University, Shenzhen, People's Republic of China

*These authors contributed equally to this work

Correspondence: Xiaoyu Liu, State Key Laboratory of Respiratory Disease for Allergy at Shenzhen University, Shenzhen Key Laboratory of Allergy & Immunology, School of Medicine, Shenzhen University, Shenzhen, People's Republic of China, Email lxy0901@szu.edu.cn

Purpose: Synthesis and characterization of silver (Ag)/titanium dioxide (TiO_2) nanocomposite (ATA) to investigate its antiviral activity against the H1N1 influenza virus and antiviral mechanisms.

Materials and Methods: A water-dispersible ATA was prepared by a photocatalytic reduction process from $AgNO_3$ and TiO_2. The characterization of ATA was performed by ultraviolet-visible spectroscopy, X-ray diffraction, high-resolution transmission electron microscopy and energy-dispersive X-ray spectroscopy. The antiviral activities and the antiviral mechanism of ATA were investigated in detail by light microscopy, transmission electron microscopy and biological techniques such as cell cytotoxicity, 50% tissue culture infectious dose detection, western blot and reverse transcription-polymerase chain reaction.

Results: These results showed the successful synthesis of ATA nanocomposite with uniform particle size and distribution. It demonstrated the highly efficient antiviral activity of ATA in a dose- and time-dependent manner, as indicated by the reduction of viral titer and the reduction of cytopathic effects caused by viral infection. In the presence of ATA, the structure of the H1N1 influenza virus is directly destroyed and even disintegrated, with the damaged surface membrane proteins and fuzzy contour. It reduces the infection efficiency of influenza by suppressing the activity and expression of hemagglutinin and neuraminidase. The results of mechanistic studies suggested that ATA nanocomposite primarily interferes with virus attachment to viral receptors on the cell surface.

Conclusion: Our study suggests that ATA may be a good antiviral candidate against the influenza virus. Compared with AgNPs alone, our synthesized ATA nanocomposites can achieve similar viral inactivation rates using only a much smaller concentration of AgNPs, greatly reducing the amount of AgNPs and their potential side effects. It has great practical value for attaching ATA to the high-efficiency particulate air network in the air purifier, which can kill the virus attached to it and limit its spread.

Keywords: silver, titanium dioxide, nanocomposites, antivirus, H1N1 influenza virus

Introduction

Influenza pandemics remain a serious public health problem worldwide. It is a major cause of seasonal epidemics and occasional pandemics that cause significant morbidity and mortality in both animals and humans due to its highly contagious and rapid transmission.[1] According to the World Health Organization, there are about one billion cases of seasonal influenza each year, including 3–5 million cases of severe illness. And it causes between 290,000 and 650,000 respiratory deaths each year.[2]

Received: 17 May 2024
Accepted: 15 October 2024
Published: 5 November 2024

The H1N1 influenza virus was first isolated from pigs in the 1930s by researchers in the United States. Subsequently, pork producers and veterinarians identified it as the cause of swine influenza infections worldwide.[3] The H1N1 influenza virus is an enveloped, negative-strand RNA virus with a segmented genome. It synthesizes and transports its components by using the machinery of the host cell.[4] Its virion is typically 80 to 120 nm in diameter and its genome contains eight segmented regions, encoding a total of 11 different proteins. The H1N1 influenza virus possesses two surface glycoproteins, hemagglutinin (HA) and neuraminidase (NA), which are determinants of virus infectivity, transmissibility, pathogenicity, host specificity, and major antigenicity. HA triggers erythrocyte aggregation by binding to sialic acid and facilitates viral attachment to infected cells, thereby enabling endocytosis.[5] NA is essential for virus budding, cleaving sialic acid receptors and promoting virus spread to neighboring cells.[6]

The antiviral drugs to treat and prevent H1N1 influenza virus infections were produced quickly. However, the effect of suppressing virus infection was only short-term because the virus is constantly mutating. Drug-resistant H1N1 strains emerged as a result of long-term use of the drugs.[7] Nowadays, it is only possible to master the dynamics of regular influenza virus mutation and to breed the new epidemic strain in time to produce a vaccine with a specific preventive effect.[8] Therefore, it is important to develop new antiviral strategies to combat wild-type and mutant influenza A virus infections.

Nanotechnology is an emerging field of applied science. Compared to larger materials, nano-sized materials are popular due to their high ratio of surface area to volume.[9] "Nanomedicine" is the application of nanotechnology for medical purposes, defined as the use of nanomaterials to diagnose, monitor, control, prevent and treat disease.[10] This includes rapid pathogen detection and biomolecular sensing,[11,12] as well as nanoparticle-based cancer therapies. Over the past few decades, a great deal of effort has been made by many researchers to study the antimicrobial properties of metal nanoparticles, and some success has been achieved.[13–15] Their application is being further extended to developing antiviral agents to inhibit various viruses.[16] Due to the advantages of high yield, good solubility and high stability, silver nanoparticles (AgNPs) have shown good activity against bacteria and fungi, and are also increasingly used as antiviral agents for the treatment of viral diseases, such as human immunodeficiency virus-1, hepatitis B virus, herpes simplex virus type 1, monkeypox virus, Tacaribe virus, also including influenza virus.[17–19] AgNPs can inhibit coronaviruses by binding to viral envelope glycoproteins and can inhibit viral penetration into host cells or inhibit the activities of NA and HA.[18,20] Recent findings have shown that AgNPs have high antiviral activity against the H1N1 influenza A virus, reducing viral titer and inhibiting viral cytopathic effect (CPE).[18]

Titanium dioxide (TiO_2) as a photocatalytic material is well known in environmental purification, carbon dioxide decomposition, and bacterial inactivation.[21] Nano-TiO_2 exhibits antibacterial activity due to the formation of reactive oxygen species (ROS) under UV light irradiation.[22] So far, photocatalytic nanomaterials including TiO_2 have been reported to be effective against a variety of viruses, such as human adenovirus GB, influenza A and B viruses, hepatitis B virus, avian influenza virus (A/H5N2) and norovirus.[23,24] Shiraki et al designed an air purifier for use in indoor environments that rapidly killed the influenza virus (A/PR/8/1934 (H1N1)) with TiO_2-coated aluminum plates and black lights mounted on a UV-led array downstream of the high-efficiency particulate air (HEPA) filter.[25] The photocatalytic activity of TiO_2 nanoparticles can be enhanced by metallic doping.[26] The antibacterial or antivirus efficiency of TiO_2 was also greatly enhanced by the incorporation of nanometals even in the absence of light.[27] Therefore, synergistic antimicrobial effect is a promising strategy for the development of improved antivirus materials.

When AgNPs were doped with TiO_2 to form nanocomposites, their cytotoxic effects on microorganisms, viruses, and cancer cells were enhanced due to the synergistic effect between AgNPs and nano-TiO_2 particles. The Ag/TiO_2 (ATA) nanocomposites can effectively eliminate bacteria belonging to both Gram-positive and negative groups.[27] Its strong antibacterial activity is mainly attributed to the synergistic effect of silver ions and ROS. Besides antibacterial properties, the ATA nanocomposites also serve as an important antiviral agent, exhibiting antiviral activity against coronavirus, SARS-coronavirus 2, HSV-1, H1N1, and enterovirus 71.[27] Basically, the ATA nanocomposites suppress the replication of viruses when in contact with them, preventing cellular respiration and ultimately leading to the death of the virus. Moongraksathum et al synthesized a series of multifunctional ATA nanocomposites with varying silver contents through the peroxysol-gel method and investigated their effective inhibitory activity against influenza A H1N1 virus and enterovirus 71.[28] It eliminates nearly 100% of the pathogens. Similar to the mechanism against bacteria, the authors suggest that the antiviral effect of ATA nanocomposites may also be generated by the synergistic action of ROS produced on the surface of TiO_2 and silver ions. However, due to a lack of data, the exact mechanism of the antiviral activity of ATA nanocomposites against the H1N1 influenza virus requires further in-depth investigation.

The main objective of this study is to prepare ATA nanocomposites by photocatalytic reduction method based on synergistic effect, and its morphology and physical characteristics were characterized by ultraviolet-visible (UV-vis), X-ray diffraction (XRD), scanning electron microscopy (SEM), high-resolution transmission electron microscopy (HR-TEM) and energy-dispersive X-ray spectroscopy (EDX). The effects of ATA on influenza virus titer, CPE caused by the influenza virus, virus structure, HA and NA protein activity and expression, the effects on eight genomes were studied in vitro to evaluate its antiviral activity against influenza virus and its antiviral mechanism. This work provides insights for a better understanding of the antiviral mechanism of ATA nanocomposites and its application to air purification systems providing important strategies for preventing the early stages of influenza virus transmission.

Materials and Methods

Preparation and Structural Characterization of ATA Nanocomposite

The ATA nanocomposite colloidal suspension was prepared by a photocatalytic reduction process from $AgNO_3$ (AR, Guangzhou Chemical Reagent Factory, Guangzhou, China, 0.226 g), TiO_2 (nano-TDA-2#, average size of 10 nm, Shenzhen Bao Shun Mei Technology Co. Ltd., Shenzhen, China, 0.54 g) and glucose (AR, Guangzhou Chemical Reagent Factory, Guangzhou, China, 4.00 g) according to the previously reported method.[29,30] Briefly, 1.00 g $AgNO_3$ was dissolved in 10 mL ddH_2O to prepare a 10% $AgNO_3$ solution. Subsequently, 4.00 g of glucose, 0.54 g of TiO_2 and 2.26 g of 10% $AgNO_3$ solution were weighed and dissolved in 100 mL of ultrapure water respectively, and then 100 mL of ultrapure water was added and stirred evenly, giving a total volume of 400 mL. Finally, the aqueous solution of ATA was obtained by a high-pressure xenon lamp (CEL-HXUV300, Beijing Zhongjiao Jinyuan Technology Co. Ltd., Beijing, China,) under the specified conditions of 300W and 15A for 30 min. The initial concentration of the ATA nanocomposite colloidal suspension in water was 1.71 mg/mL (ie, 0.36 mg/mL of Ag and 1.35 mg/mL of TiO_2). Before cell testing, samples were sterilized by eliminating bacteria through the 0.22 μm membrane filters.

The UV-vis absorption spectrum of the ATA colloid solution ranging from 200 to 800 nm was analyzed using a UV-vis spectrophotometer (UV-2550, Shimadzu, Japan). The surface morphology and particle sizes of the ATA nanoparticles were observed using SEM (S4800, Hitachi, Japan) and HR-TEM (Tecnai G20, FEI, USA) equipped with EDX devices with an accelerating voltage of 200 kV. A small amount of ATA colloid solution was added to the conductive adhesive to prepare an SEM sample, which was quickly dried and sprayed with gold for SEM observation. The TEM samples were prepared by placing a drop of a dilute colloidal dispersion of ATA on the surface of a 400-mesh copper grid coated with formvar and drying in a vacuum chamber for 1 h. Part of the solution was freeze-dried for further XRD (D8 Advance, Deutsche Bruker GmbH, German) testing of ATA. A Cu Ka radiation (40kv, 300mA) source is used for XRD detection with a scan speed of 12°/min and a scan angle range of 20°-80°.

Cells and Virus

The human influenza A virus (A/Puerto Rico/8/1934 (H1N1)) was kindly provided by the State Key Laboratory of Respiratory Disease, the First Affiliated Hospital of Guangzhou Medical University. The viruses were passed into 10-day-old embryonated chicken eggs. The virus-containing allantoic fluid was harvested and stored at −80°C until use. The infectivity of the influenza virus was tested in Madin-Darby canine kidney (MDCK, ATCC, NBL-2) cells purchased from the American Type Culture Collection. Dulbecco's modified Eagle's medium (DMEM, C11995500BT, Gbico, USA, 500 mL) supplemented with 10% fetal bovine serum (FBS, A5670701, Gbico, USA, 500 mL) was used for MDCK cell culture.

The 50% Tissue Culture Infectious Dose ($TCID_{50}$) assay is a viral titration experiment that can be used to quantify virus titers by investigating the CPE of a virus on an inoculated host cell culture.[31] Briefly, the MDCK cells growing overnight in the 96-well tissue culture plates were washed once with sterile Dulbecco's phosphate-buffered saline (DPBS, C11995500BT, Gbico, USA, 500mL). The virus was ten-fold serial dilution and inoculated into MDCK cells at 37 °C and 5% CO2 for 2 h. After 2 h of uptake, the new DMEM culture medium containing 1.5 μg/mL TPCK trypsin (SIGMA, 4370285, USA) was replaced for further culture. The $TCID_{50}$ was calculated using the Reed-Muench method based on the CPE after 48 or 72 hours.[32]

Cytotoxicity Test

The cytotoxicity of ATA, Ag and TiO_2 nanomaterials to the MDCK cells was measured by using the MTT assay (Solarbio, M1020, 500T, Beijing Suolaibao technology CO. LTD; Beijing, China). Briefly, the three nanomaterials were serially diluted two-fold and inoculated into the cells in the 96-well plates. After 2 days of cultivation, the solutions were replaced with 100 μL DMEM solution containing 10 μL of MTT solution for an additional culture of 4 h. Finally, to dissolve the formazan crystals, 110 μL of the formazan dissolving solution was added to each well and the optical density was measured at 490 nm in an enzyme-linked immunosorbent assay instrument after a brief shock.

Assay for Influenza Virus Inactivation Rate

The ATA was diluted with sterile ddH_2O to 512, 256, 128, 32 and 8 μg/mL, respectively. The mixtures of virus (0.1 mL, $lgTCID_{50}$=6.5) with different concentrations of ATA (0.1 mL) or sterile ddH_2O control were prepared and maintained at room temperature for a period of time. The final action concentrations were 256, 128, 64, 16 and 4 μg/mL, respectively. After the treatment for 5, 10, 30 or 60 min, 0.8 mL DMEM was added and the mixtures were centrifuged at 6000 rmp for 5 min to wipe off the ATA. The antiviral activity of ATA was then determined by comparing the $lgTCID_{50}$ between the treatment groups and the virus control groups as described above. In addition, to compare the antiviral activity of ATA and its composites (Ag and TiO_2), their antiviral activities against the H1N1 influenza virus at a concentration of 5 μg/mL were also studied. All experiments were repeated three times to calculate the average virus inactivation rate:

$$R_1(\%) = \frac{A_1 - B_1}{A_1} \times 100 \quad (1)$$

Where R_1 is the average virus inactivation rate, A_1 is10^ The average virus inactivation negative logarithm of the control group, and B_1 is10^ The average virus inactivation negative logarithm of the experimental group.

The Direct Inhibitory Effect of ATA on Influenza Virus

Different concentrations of ATA nanomaterials were added to the same volume of $200TCID_{50}$ virus solution. After treatment at room temperature for 30 min, the mixtures were centrifuged at 6000 rmp for 5 min. 100 μL of the supernatants were removed and incubated on MDCK cells at 37 °C in 5% CO_2 for 2 h to allow viral infection of the MDCK cells. The inoculum was removed after 2 h and replaced with fresh DMEM culture medium containing 1.5 μg/mL TPCK trypsin, and the culture was continued for 48 h. The CPE was observed by an inverted microscope and the inhibition rate was calculated according to the following formula based on the cell viability detected by MTT assay.

$$R_2(\%) = \frac{A_2 - B_2}{C_2 - B_2} \times 100 \quad (2)$$

Where, R_2 is the inhibition ratio, A_2 is OD490 of the experimental group, B_2 is OD490 of the virus control group, and C_2 is OD490 of the normal control group.

Negative Staining TEM

The H1N1 viruses were treated with different concentrations of ATA nanomaterials for 30 min. The TEM samples were added to copper mesh and negatively stained with 3% phosphotungstic acid (pH 7.0) for 2 min. The copper mesh was observed using a TEM (H7650, Hitachi High-Technologies Corporation, Tokyo, Japan).

Hemagglutinin Inhibition (HI) Test

HA titer and HI tests were performed according to the World Health Organization Manual on Animal Influenza Diagnosis and Surveillance.[33] The 0.5% chicken erythrocytes suspended in PBS were used for the HA and HI tests in 96-well microplates with V-shaped bottoms. For HA titration, ATA-treated or untreated viruses were serially diluted two-fold in PBS. After adding 50 μL of virus solution to each well, an equal volume of 0.5% chicken erythrocytes was added. Plates were kept at room temperature and results were observed after 45 min. The HA titer was expressed as the maximum dilution of the virus that produced complete HA.

For the HI test, the HA titer was determined as described above and the virus containing 8 HA units was diluted in PBS. Plates containing a mixture of 25 μL of virus containing 8 HA units and 25 μL of different concentrations of ATA were incubated for 30 min. After treatment, 50 μL of 0.5% chicken erythrocytes were added. The results were observed and recorded after 45 min. The chicken erythrocytes treated with ATA alone without the virus were used as controls.

NA Test

The NA activity of the virus was measured using the NA assay kit (Beyotime, P0306, 100T, Beyotime Biotechnology, Shanghai, China). Briefly, 10 μL of the sample solutions were added into the detection system and incubated at 37°C for 30 min. The NA activity was reflected by the intensity of fluorescence emitting an emission wavelength of 440 nm at an excitation wavelength of 360 nm. At the same time, negative and positive controls were established.

Western Blotting (WB) Assay

To further investigate the mechanism of viral inactivation by ATA, a WB assay was used to detect the effects of ATA on the HA and NA proteins of the influenza virus. Total viral proteins were harvested directly from the viral supernatant. SDS-PAGE electrophoresis was then performed. After proteins were transferred to polyvinylidene difluoride membrane (PVDF, Invitrogen, LC2005, Waltham, USA) at 300 mA for 1 h at 4°C, the membrane was blocked for 2 h with 3% skim milk (Biosharp, BS102-500g, Beijing, China) dissolved in Tris-Buffered Saline Tween-20 (TBST, Biosharp, BL315B, Beijing, China) buffer. The membrane was then washed five times with TBST buffer for 5 min each time. The TBST buffer was drained off and the influenza A virus H1N1 HA antibody (Gene Tex, GTX12735, California, USA) or NA antibody (Gene Tex, GTX636323, California, USA) was added and incubated overnight at 4°C. The horseradish peroxidase-conjugated secondary antibodies (Abcam, ab205718, Cambridge, UK) were incubated for 60 min. The complexes were detected using a western illumination chemiluminescence system (UVITEC, HD6, Cambridge, UK).

Reverse-Transcription Polymerase Chain Reaction (RT-PCR)

Viral polymerase basic protein 2 (PB2), polymerase basic protein 1 (PB1), polymerase acidic protein (PA), nucleoprotein (NP), matrix protein (M), non-structural protein (NS), HA and NA genes were amplified from the A/Puerto Rico/8/1934 H1N1 virus treated with ATA nanomaterials by RT-PCR. The QIAamp Viral RNA Kit (QIAGEN, 52904, Hilden, Germany) was used to extract treated or untreated viral RNA. The OneStep RT-PCR kit (TAKARA, P0306, Takara Bio Inc. Japan) was used to detect all of the eight H1N1 virus genes: PB2, PB1, PA, HA, NP, NA, M and NS. The primer sets of the eight genes of H1N1 are shown in Table 1.

Table 1 The Primer Sets of the Eight Genes of H1N1 Table 1

Primer	Primer sequence (5'to3')	Length
PB2_F	TGTAAAACGACGGCCAGTAGCRAAAGCAGG	2300
PB2_R	CAGGAAACAGCTATGACCCGTTTYCKTTTCATYACCAACAC	
PB1_F	TGTAAAACGACGGCCAGTAGCRAAAGCAG	2300
PB1_R	CAGGAAACAGCTATGACCAGTAGRAACAAGGCATT	
PA_F	TGTAAAACGACGGCCAGTAGCRAAAGCAG	2300
PA_R	CAGGAAACAGCTATGACCAAACAAKGTACTTTTTTGGACAG	
HA_F	TGTAAAACGACGGCCAGTAGCRAAAGCAGGGAAA	1770
HA_R	CAGGAAACAGCTATGACCAGTAGAAACAAGGGTG	
NP_F	TGTAAAACGACGGCCAGTAGCAAAAGCAGGGTAG	1552
NP_R	CAGGAAACAGCTATGACCTTTCHTYAATTGTCRTACTCCTC	
NA_F	TGTAAAACGACGGCCAGTAGCRAAAGCAGGAG	1440
NA_R	CAGGAAACAGCTATGACCTTTTCAACGRACTACTTGTCAATG	
MP_F	TGTAAAACGACGGCCAGTAGCRAAAGCAG	1014
MP_R	CAGGAAACAGCTATGACCTAGTTTTTTACTCYAGCWCTATG	
NS_F	TGTAAAACGACGGCCAGTAGCRAAAGCAGGG	873
NS_R	CAGGAAACAGCTATGACCTTTTATYAYTAAATAAGCTGAAABG	

Cycling conditions included a reverse transcription step (50 °C for 15 min). The PCR reaction included an initial denaturation step (94 °C for 2 min), followed by a cycle of denaturation (94 °C for 30s), annealing (50 °C for 15s) and extension (72 °C for 1 min) for 35 cycles, with a final extension at 72 °C for 10 min. Products were detected by 1% agarose gel electrophoresis.

Statistical Analysis

The experimental results were repeated three times. The data were expressed as mean values and statistically analyzed by Graph Prism. *T*-test was used between the experimental group and the control group, A significance level of *P < 0.05 was deemed statistically significant, **P < 0.01 and***P < 0.001 and ****P < 0.0001 were considered highly significant, while ns was deemed there was no difference compared with the control group.

Results

Fabrication and Characterization of ATA

ATA nanoparticles were prepared by a photocatalytic reduction process. Under UV irradiation, the color of the solution changed from colorless to brown as depicted in Figure 1A. Afterward, the UV-vis spectra of ATA and $AgNO_3/TiO_2$ colloid dispersions were examined. An absorption band appears at 410 nm in the ATA colloidal dispersion (red curve), whereas there was no significant absorption at this frequency in the $AgNO_3/TiO_2$ colloid (black curve) as shown in Figure 1B. This strong absorption is most likely due to the surface plasmon resonance of Ag0 metal nanocrystals,[34] indicating the successful formation of ATA nanoparticles. The morphology of the synthesized ATA nanoparticles was initially evaluated using SEM. The result depicted in Figure 1C shows that the ATA nanocomposites exhibited

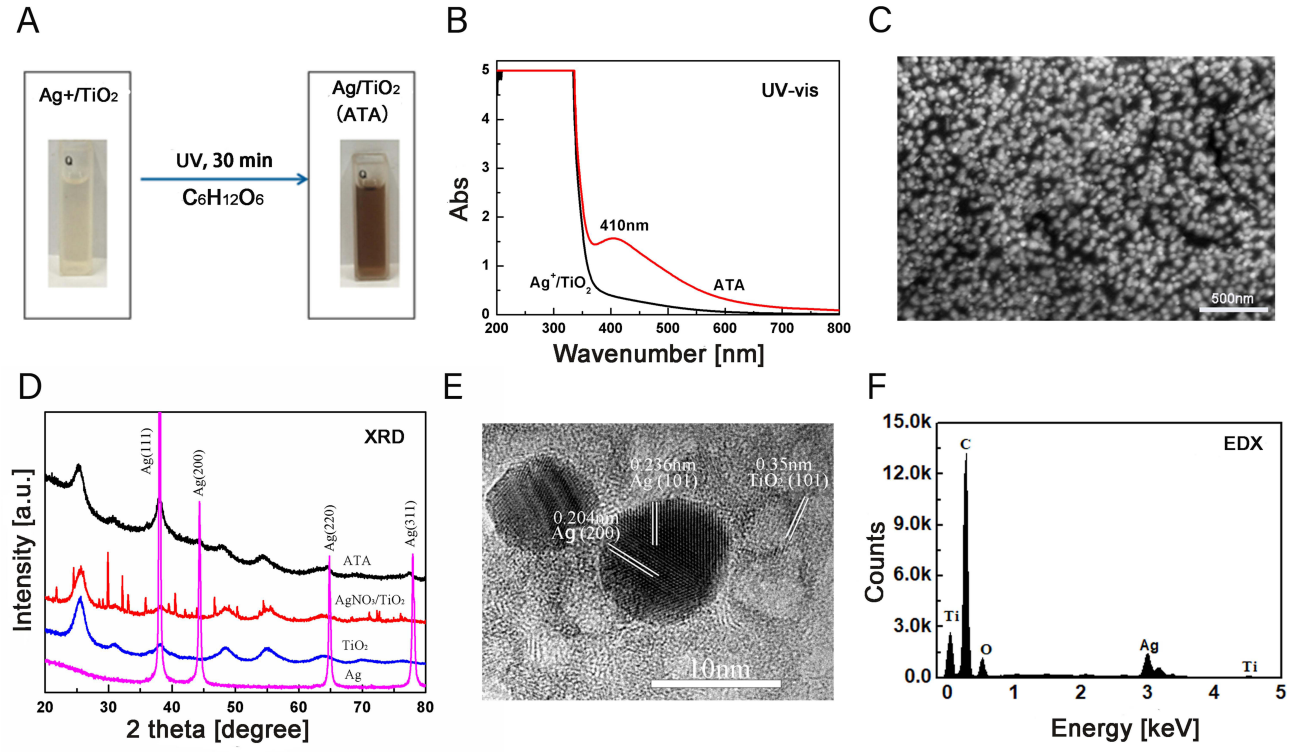

Figure 1 Fabrication and characterization of ATA nanocomposites. (**A**) ATA nanocomposites were prepared by a photocatalytic reduction process. Under ultraviolet irradiation, the color of the solution changed from colorless to brown. (**B**) Ultraviolet-visible absorption spectra of the ATA and $AgNO_3/TiO_2$ colloid dispersions were examined. An absorption band appears at 410 nm in the ATA colloidal dispersion (red curve), whereas there was no significant absorption at this frequency in the $AgNO_3/TiO_2$ colloid (black curve). (**C**) Scanning electron microscopy results depicted that the ATA nanocomposites exhibited a relatively uniform particle size and distribution. (**D**) The X-ray diffraction pattern of the ATA indicates that the TiO_2 occurs as anatase (JCPDS: 21–12,726). The characteristic peaks for Ag (JCPDS:04–0783) located at 38.12° (111), 44.28° (200), 64.43° (220) and 77.40° (311) were found in ATA. (**E**) High-resolution - transmission electron microscopy image showed that the nanoparticles exhibited a high degree of crystallinity, as indicated by the well-resolved Ag (101), Ag (200), and TiO_2 (101). Scar bar: 10 nm. (**F**) ATA nanocomposites investigated by energy-dispersive X-ray spectroscopy showed that the component elements of ATA were C, O, Ti, and Ag. (ATA: Ag/TiO_2; Ag: Silver; TiO_2: Titanium dioxide).

a relatively uniform particle size and distribution. The XRD pattern (Figure 1D) of the ATA nanoparticles indicates that the TiO_2 occurs as anatase (JCPDS: 21–12,726). The characteristic peaks for Ag (JCPDS:04–0783) located at 38.12° (111), 44.28° (200), 64.43° (220) and 77.40° (311) were found in Ag and ATA. The corresponding HR-TEM image (Figure 1E) showed that the nanoparticles exhibited a high degree of crystallinity, as indicated by the well-resolved Ag (101), Ag (200) and TiO_2 (101). The elemental composition of the ATA nanocomposites investigated by EDX showed that the component elements of ATA were C, O, Ti and Ag (Figure 1F), further indicating the successful formation of ATA nanoparticles.

Cytotoxicity

MDCK cells are commonly used to detect the titer of influenza virus. Therefore, we first examined the cytotoxicity of the three materials against MDCK. The cytotoxicity of the three types of nanomaterials was determined by two-fold serial dilution from the initial concentration. As shown in Figure 2A, the maximum non-toxic concentrations are 26.72 μg/mL (ATA) and 5.63 μg/mL (Ag), respectively. However, the TiO_2 was less toxic with a maximum non-toxic concentration of 337.5 μg/mL, indicating that Ag mainly caused the toxicity of ATA.

Inactivation of the A/Puerto Rico/8/1934 H1N1 Virus by ATA

The antiviral activity of the ATA composites was estimated as the $TCID_{50}$ of the ATA-treated supernatant to the control (untreated) viral suspension. As shown in Figure 2B, the different concentrations of ATA showed different degrees of antiviral effect on the influenza virus under different action times. The high concentration of ATA has a good antiviral effect in a short time. For example, at a concentration of 128 or 256 μg/mL, the virus-inactivating rate can reach more than 90% in 5 or 60 min. However, the average virus inactivation rate decreased slightly at the concentration of 64 μg/mL.

Although ATA at low concentration (4, or 16 μg/mL) did not show ideal virus-inactivating ability in a short period, the average virus inactivation rate was less than 50% at 5 min (12.90%, 22.38%) and 10 min (22.38%, 30.82%) incubation times. However, the rate of virus inactivation could be significantly increased by prolonging the treatment time. The mean virus inactivation rates of ATA reached 54.29% (4 μg/mL) and 64.52% (16 μg/mL) at 30 min incubation times. When the antiviral activity of ATA was tested with longer treatment for 60 min, the mean virus inactivation rates reached 68.38% (4 μg/mL), 78.62% (16 μg/mL) and 95.32% (64 μg/mL). These results show that ATA exerts antiviral activity in vitro in a time- and dose-dependent manner.

For comparison, the antiviral effects of ATA, Ag and TiO_2 at the same concentrations of 5 μg/mL were all detected (Figure 2C). With a treatment time of 60 min, the average virus inactivation rates were 72.46% (ATA), 62.46% (Ag) and 12.90% (TiO_2), respectively. Obviously, the antiviral effect of ATA is slightly stronger than that of Ag, whereas TiO_2 has a negligible antiviral effect. The results showed that Ag rather than TiO_2 was the major component of ATA that exerted antiviral activity. In addition, 5 μg/mL ATA containing Ag concentration was 1.053 μg/mL, which reduced the amount of Ag and reached a higher killing ability of the influenza virus.

The direct treatment mode was also used to assess the direct inhibitory effect of ATA on the H1N1 influenza virus. The cell degeneration caused by virus infection of tissue culture cells is referred to as the CPE. The ability of the virus to infect cells was measured by the degree of CPE in infected cells and the calculated inhibition rate of the virus as measured by the MTT assay for cell viability. The MTT assay (Figure 2D) demonstrated that the cell viability of the virus control was only 32.72%. After treatment with 4, 16 and 64 μg/mL of ATA, the cell survival rate of ATA rose to 49.57%, 73.91% and 84.72%, respectively. The cell survival rates of ATA were achieved at 87.81% and 96.59% at 128 and 256 μg/mL, respectively. Furthermore, virus-infected cells treated with various concentrations of ATA exhibited distinct levels of CPE. As shown in Figure 2E, the virus treated with 4 μg/mL ATA had a similar infection, reaching almost 100% CPE. The viral CPE reduced to approximately 75% and 50% for treatments of 16 μg/mL and 64 μg/mL ATA, respectively. In the presence of 128 μg/mL ATA, less than 25% CPE was observed. At 256 μg/mL, the cells were the same as the normal control without CPE. These findings imply that ATA can inhibit the cellular infection of influenza virus.

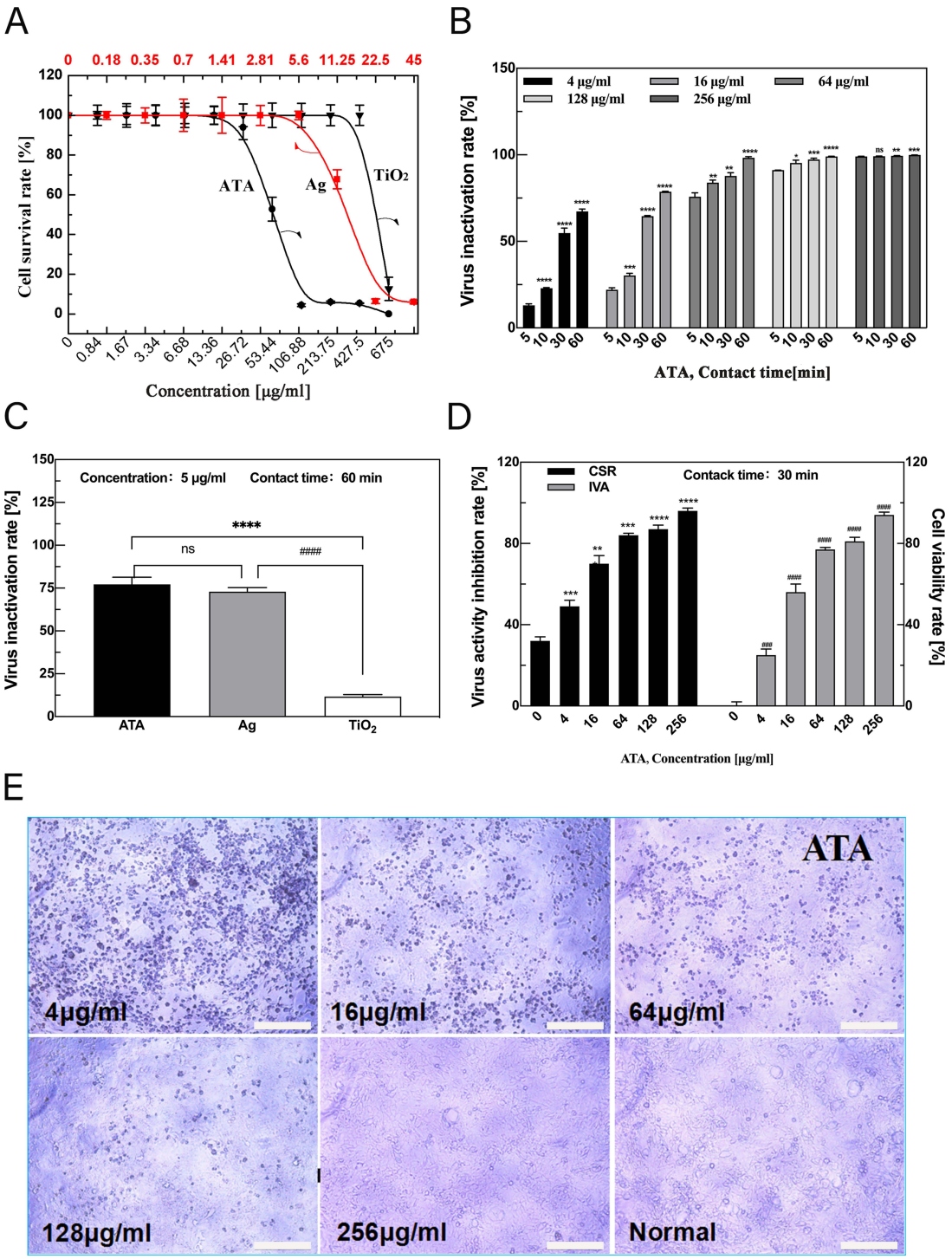

Figure 2 ATA nanocomposites exert potent antiviral activity in a time- and dose-dependent manner. (**A**) Cytotoxicity of TiO_2, Ag and ATA nanoparticles with different concentrations against Madin–Darby canine kidney cells. The maximum non-toxic concentrations of ATA and Ag were 26.72 μg/mL and 5.63 μg/mL, respectively. (**B**) Virus inactivation rates of ATA at different concentrations (4,16,64,128,256 μg/mL) with different processing times (5, 10, 30, 60 mins). The ATA nanocomposites exert potent antiviral activity in a time- and dose-dependent manner. *p < 0.05, **p < 0.01, ***p < 0.001 ****p < 0.0001 vs the 5-min action time group under the same concentration, respectively, NS, not significant. (**C**) Comparison of virus inactivation rates of Ag, TiO_2, and ATA. The experiments measured at the same concentration of 5 μg/mL with the treatment of 60 minutes showed that the average virus inactivation rates of ATA, Ag, and TiO_2 are 72.46%, 62.46%, and 12.90%, respectively. ****p < 0.0001 vs the ATA group, $^{\#\#\#\#}$p < 0.0001 vs the Ag group, NS, not significant between ATA and Ag. (**D**) Virus inhibition rate of different concentrations as a direct mode of ATA by MTT with 60 mins treatment. ATA improves CSR and IVA caused by influenza virus infection in a dose-dependent manner. **p < 0.01, ***p < 0.001 ****p < 0.0001 vs Control group (0 μg/mL) of CSR. $^{\#\#}$p < 0.01, $^{\#\#\#}$p < 0.001 $^{\#\#\#\#}$p < 0.0001 vs Control group of IVA. (**E**) ATA reduced the cytopathic effect caused by influenza virus infection in a dose-dependent manner. Scar bar: 100 μm. (ATA: Ag/TiO_2; Ag: silver; TiO_2: titanium dioxide; CSR: cell viability rate; IVA: virus activity inhibition rate).

The Direct Damage to the Virus Structure of ATA Observed by TEM

To further develop a mechanistic understanding of ATA's inactivation of H1N1 viruses, we examined the control (untreated) and treated virus suspension samples using a TEM. Influenza virus particles are approximately 80–120 nm in diameter, roughly spherical in shape, and can be structurally divided into three layers. The outer layer of the bilayer lipid membrane contains mainly three protrusions on the protein, including HA, NA and small amounts of M2 proteins. The lipid membrane contains a layer of M1 protein that surrounds the ribonucleoprotein core. The normal virion has a complete structure as described. However, we can easily see the difference between control and treated virus particles as shown in Figure 3. Viral particles exposed to ATA show an incomplete structure with ill-defined, faintly outlined and missing surface peaks. Different concentrations of ATA cause different degrees of virus destruction. Compared to the untreated virus (0 μg/mL), 4 μg/mL: the virus envelope was not damaged and its structure was intact; 16 μg/mL: the virus envelope was slightly damaged and 2 swollen bulges or cleavages were found (see red arrowhead in the picture); 64 μg/mL: the envelope of the virus was severely damaged and there were many swollen bulges or fissures (see red arrow in the picture); 128 μg /mL: although the virus has a holistic form, the envelope is completely damaged, without a membrane. At 256 μg/mL, the virus even disintegrates, making it difficult to find structurally intact virus particles in our viewing field.

Effect of ATA on H1N1 Virus HA and NA

NA and HA are not only two important glycoproteins on the structural envelope of the influenza virus but also play important roles in the replication cycle of the influenza virus. The effect of ATA on the H1N1 virus HA and NA was first understood by detecting the activity of HA and NA. As shown in Figure 4A, the activities of NA were slightly decreased at concentrations below 64 μg/mL. But it has a significant decrease from 40000 to 30000 and 14600 at 128 and 256 μg/mL, respectively.

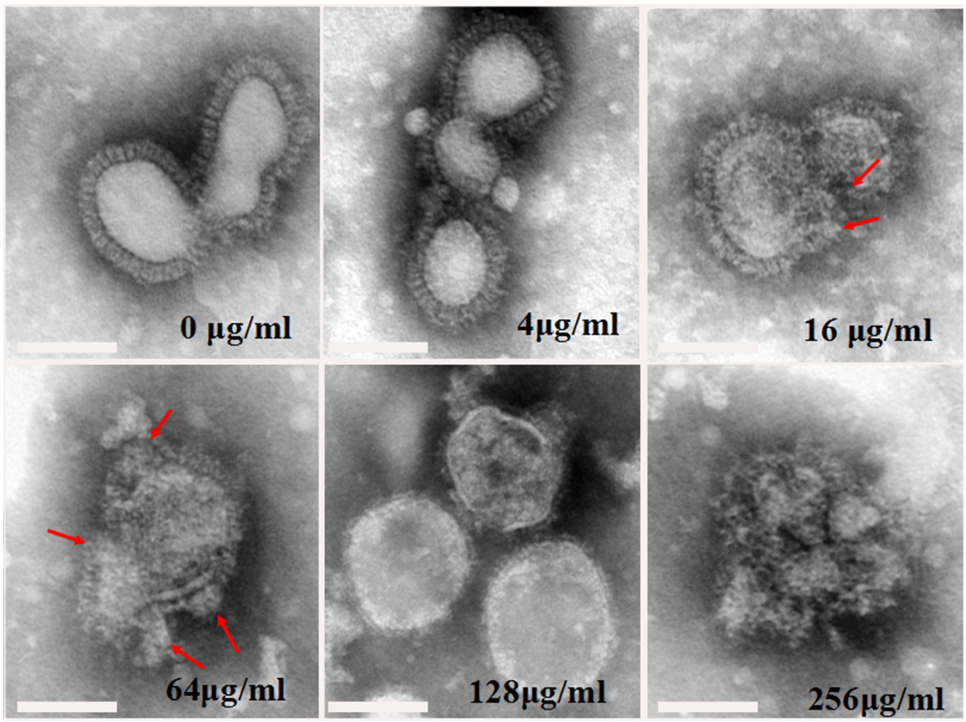

Figure 3 The direct damage to the virus structure of ATA was observed by TEM. TEM images showing the different degrees of damage to virus structure with the treatment of 30 min at different concentrations of ATA. Compared to the untreated virus (0 μg/mL), 4 μg/mL: the virus envelope was not damaged and its structure was intact; 16 μg/mL: the virus envelope was slightly damaged and two swollen bulges or cleavages were found (see red arrowhead in the picture); 64 μg/mL: the envelope of the virus was severely damaged and there were many swollen bulges or fissures (see red arrow in the picture); 128 μg/mL: although the virus has a holistic form, the envelope is completely damaged, without a membrane. At a concentration of 256 μg/mL, the virus even disintegrates, making it difficult to find structurally intact virus particles in our viewing field. Scar bar: 100 nm. (ATA: Ag/TiO_2; TEM: transmission electron microscopy).

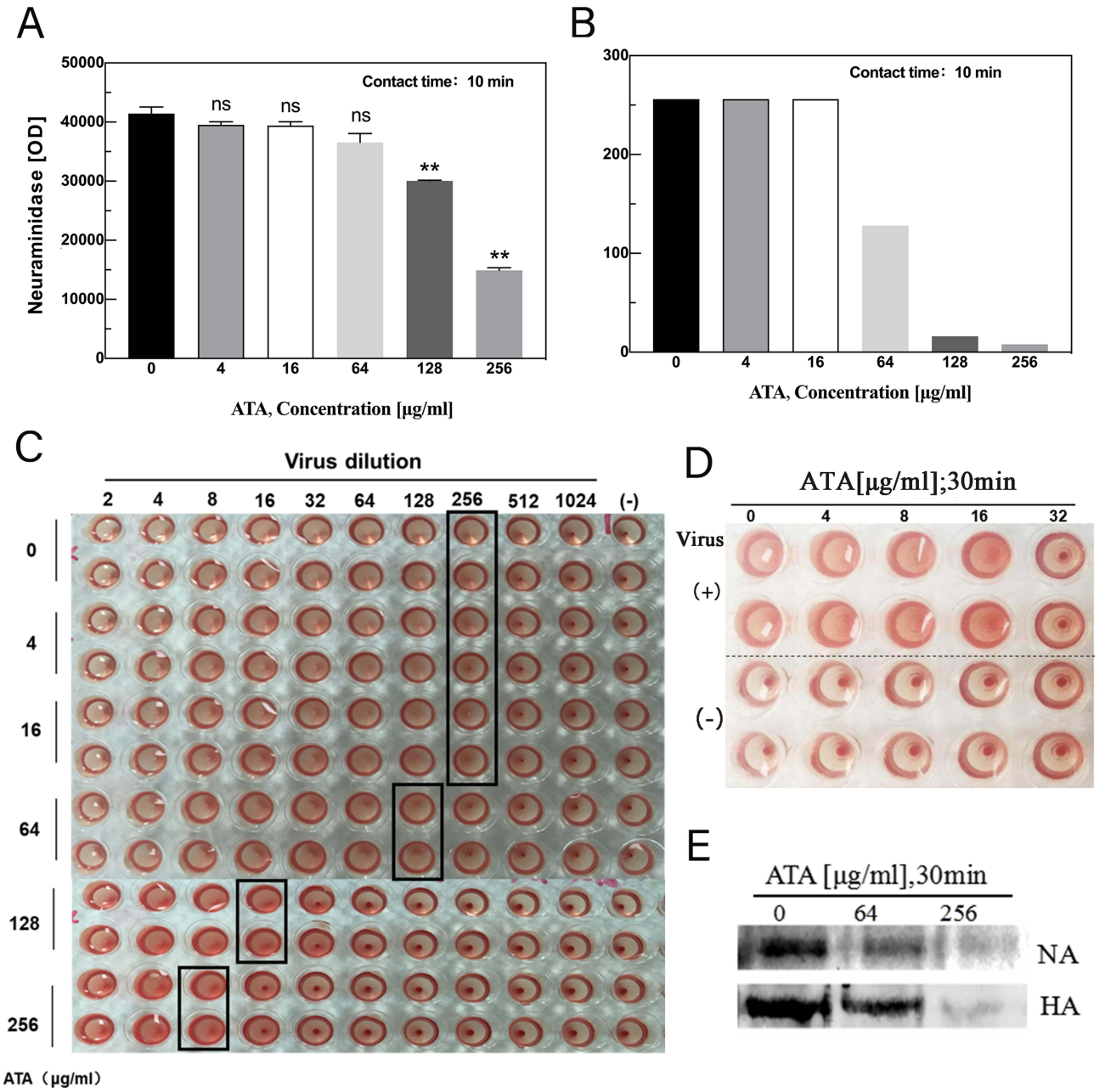

Figure 4 Effect of ATA on H1N1 virus NA and HA. (**A-C**) The influence of ATA on NA and HA activity of H1N1 virus with the treatment of 10 min; (**A**) NA activity did not change significantly under low concentrations of ATA, but decreased from 40000 to 30000 and 14600 under high concentrations of 128 μg/mL and 256 μg/mL, respectively. **p < 0.01 vs Control group (0 μg/mL), NS, not significant. (**B** and **C**) The effect of ATA on influenza virus HA activity was determined by measuring the HA titer of in chicken red blood cells. As shown in B and C, the HA titer of the virus control strain without ATA treatment was 256. The HA titer of 4 μg/mL and 16 μg/mL ATA-treated virus were the same as the viral control. However, at a concentration of 64 μg/mL, the HA titer was dropped to 128 and even to 16 and 8 at 128 μg/mL and 256 μg/mL, respectively. (**D**) Viruses with HA titers of 512 were used for NA inhibition assays of ATA nanomaterials at different concentrations. The results showed that the ATA at 32 μg/mL can inhibit the hemagglutination of influenza virus. (**E**) Dependence of Western blotting showing the expression of NA and HA proteins of untreated or treated virus. The test was measured with a treatment of 30 min. At a concentration of 64 μg/mL, the expression of NA protein was significantly decreased. When the concentration was 256 μg/mL, neither HA nor NA protein was expressed. (ATA: Ag/TiO_2; HA: hemagglutinin; NA: neuraminidase).

At the experimental time of treatment, the HA titer of the virus control strain without ATA treatment was 256. The HA titer of 4 μg/mL and 16 μg/mL ATA-treated virus were the same as the viral control. However, at a concentration of 64 μg/mL, the HA titer was dropped to 128, and it was even reduced to 16 at 128 μg/mL and 8 at 256 μg/mL (Figure 4B and C). The HI assay was performed on different concentrations of ATA nanomaterials using a virus with an HA titer of 512. The results showed that the minimum inhibition concentration of ATA was 32 μg/mL, which was not toxic to

chicken erythrocytes (Figure 4D). Actually, we have performed the effect of individual ATA on chicken erythrocytes before the HI assay and showed that ATA up to 256 μg/mL did not affect chicken erythrocytes (Figure S1A). These results exclude the effect of ATA on chicken erythrocytes and further suggest that ATA has a direct inhibitory effect on HA of the H1N1 influenza virus.

To further investigate the effect of ATA on these surface proteins, the WB assay was performed on ATA-treated viruses (Figure 4E). Similar to the results of HA and NA activities, WB analysis showed that ATA significantly affected the protein expression of NA and HA. ATA at the concentration of 64 μg/mL slightly inhibited the expression of HA protein. The effect of ATA on NA protein was greater than that on HA protein. At the concentration of 64 μg/mL, the expression of NA protein was significantly decreased. When the concentration reached 256 μg/mL, neither HA nor NA proteins were expressed. These results suggest that ATA may affect the adsorption of the influenza virus to host cells and hinder the replication of the influenza virus by disrupting the membrane structure of the influenza virus and disrupting the membrane protein activity.

Detection of H1N1 Viral Genes by RT-PCR

These viral genes were amplified by RT-PCR from A/Puerto Rico/8/1934 H1N1 virus treated or not with ATA. However, no profound damage to the viral genes was observed (Figure S1B). This indicated that ATA did not cause damage to the viral genome.

Discussion

Nanoparticles in the size range of 1–100 nm have mostly been used for virus inhibition.[35] AgNPs were reported to have antiviral activity against various viruses. It is reported that AgNPs have antiviral activity against the influenza virus and can significantly reduce the viral titer in vitro, inhibit CPE, disrupt the structure of the influenza virus, and rapidly inhibit the hemagglutination of influenza virus to chicken erythrocytes. The results of the mechanism study suggest that AgNPs bind to the viral envelope glycoprotein, thereby preventing the virus from penetrating host cells, and can also enter cells and interact with the viral genome (DNA or RNA) or inhibit viral replication to exert their antiviral activity.[36] Although the antiviral activity of Ag nanoparticles against the influenza virus has been recognized, the effect of ATA against the influenza virus has rarely been discussed. Moongraksathum et al have synthesized ATA nanocomposites by the peroxo sol-gel method and have demonstrated high antiviral activity against the influenza virus, but the exact mechanism is not yet clear.[28] ATA nanocomposites can be prepared by various methods, including impregnation, sol-gel, co-precipitation, hydrothermal, photo deposition, and chemical reduction techniques. Among these methods, chemical reduction is one of the simplest techniques for producing ATA nanoparticles with controlled size, shape, and good dispersion. We successfully prepared ATA nanocomposites with uniform and evenly distributed nanoparticles using the chemical reduction method and conducted an in-depth analysis of their antiviral activity and specific action mechanisms.

In the present study, we performed antiviral assays using the influenza virus (A/Puerto Rico/8/1934 (H1N1)) to evaluate the antiviral ability of ATA. ATA synthesis by photocatalysis reaction rapidly and effectively inactivated the H1N1 influenza virus at high concentrations (128 or 256 μg/mL). It can inactivate more than 90% of the virus within five minutes. None of the lower concentrations of ATA showed significant antiviral activity against the H1N1 influenza virus within a short period. However, the average virus inactivation rates were significantly improved by prolonging the duration of action. These results suggest that ATA effectively reduces the viral titer of the influenza virus in a dose and time-dependent manner. These observations appear to be similar to the previous study on the antiviral effect of AgNPs on H1N1 influenza, which showed a concentration-dependent anti-H1N1 influenza A virus effect of AgNPs.[18]

To further investigate the effect of ATA on the structure of the H1N1 influenza virus, the ATA-treated viruses were analyzed under the TEM to observe their morphology. We can easily see the big differences between treated and untreated viruses. A normal influenza virus particle has a typical and complete structure, as shown in Figure 3. However, it was found that most of the structures observed in the treated virus were poorly defined, these structures appeared to be faintly outlined and lacking in surface peaks. The discovery of a large number of morphologically abnormal virus particles from the treated H1N1 virus suggests that the structural changes may be associated with the anti-viral effect of ATA. The similar structural damage of the virus particles was also found in the H9N2 virus treated with copper-iron and

CuZeo textiles.[35,37] Since the destruction of proteins in the outer layer of the influenza virus by ATA was observed by TEM, further studies were carried out to demonstrate the inactivation activity of ATA on important envelope proteins, including the transmembrane glycoproteins: HA and NA, both of which play critical roles throughout the viral life cycle. Influenza virus enters the cell by endocytosis via HA binding to sialic acid-containing glycoprotein receptors on the cell surface.[38] In this study, the HA titers of the H1N1 viruses were significantly reduced after treatment with ATA. Compared with the 256 titers of the control virus, the viral HA titers in the ATA nanoparticle groups were below 8. Our results show that ATA nanoparticles can inhibit the HA activity of chicken erythrocytes with the H1N1 influenza A virus.

The HI results showed that in the presence of ATA nanoparticles at a concentration of 32 μg/mL, the ability of the H1N1 influenza A virus with 8 HA units to agglutinate chicken erythrocytes was completely inhibited. These results suggest that ATA nanoparticles play a critical role in blocking the binding of the H1N1 influenza A virus to erythrocytes and inhibiting the viral entry process. As reported, the same result showed that the ability of the H1N1 influenza A virus to agglutinate the erythrocytes was inhibited in the presence of AgNPs.[20] In other similar research, they have not found this difference in the influenza virus treated with HT or with CuZeo textiles.[35,39] Just as important as HA is NA, the abundant glycoprotein on the surface of influenza viruses. It has an enzymatic activity that promotes the release of viral progeny from a host cell during the final stage of viral replication and the spread of infection to new cells.[40] NA activity can be inhibited with specific inhibitors, such as zanamivir and oseltamivir carboxylate, and then reduce the efficiency of virus infection of host cells,[41] but the drugs developed resistance to the virus due to the single target and long use. In the presence of ATA nanoparticles, the NA activity was significantly inhibited. To further confirm the effect of ATA nanoparticles on the NA and HA of the influenza H1N1 virus, the results of WB showed that the expression of the NA and HA proteins was significantly reduced compared to the control group. HA and NA are responsible for the binding to and releasing from host cell receptors, they are crucial for the determination of host specificity. It is suggested that in addition to interfering with HA, ATA nanoparticles may also reduce the infection efficiency of influenza virus by interfering with viral NA activity.

One study reported that HT (a small-molecule phenolic compound) can effectively reduce enveloped viruses in a dose-dependent manner,[42] but it did not affect the titer of all non-enveloped viruses tested. It has been suggested that the viral envelope may be involved in the mechanism of antiviral action. In our study, a series of results showed that ATA nanoparticles disrupted the viral structure, inhibited NA and HA activity, and reduced the expression of NA and HA proteins, as shown in Figure 5 of the schematic of the antiviral mechanism of ATA. This is important because both NA and HA are the major surface membrane proteins of the influenza H1N1 virus. Together, they form the outermost structure of the virion. It was likely that ATA nanoparticles process a similar mode of antiviral action, they exert an antiviral effect on the influenza virus by acting on H1N1 viral member structure. In our study, ATA nanoparticle treatment did not have any effect on H1N1 virus genes. Because ATA nanoparticles interact primarily with the viral surface, they are more likely to damage viral envelope proteins than viral nucleic acids.

The antibacterial and antifungal mechanisms of AgNPs are thought to depend on the release of Ag ions, which strongly inhibit their growth by suppressing respiratory enzymes and electron transport components and by interfering with DNA functions.[43,44] In contrast to their antibacterial and antifungal activities, the main antiviral mechanism results mainly from the direct binding of AgNPs to viral envelope glycoproteins and inhibition of virus attachment to host cells. Orlowski et al showed that tannic acid-modified AgNPs interacted with the surface glycoproteins of herpes simplex virus-2.[45] With antiviral activity against HIV, AgNPs also inhibit virus-cell attachment by interacting with the gp120 protein of HIV.[46] Therefore, AgNPs primarily interfere with virus attachment to viral receptors on the cell surface rather than viral nucleic acids. The envelope of the influenza virus primarily originates from the host cell membrane, and its function is to help the virus enter the host cell. Each HA molecule has two disulfide bonds that can be broken to expose receptor binding sites that can interact with host cells.[47] These exposed disulfide bonds may be binding sites for ATA to interact with the virus, and thus they exhibit antiviral activity when the receptor binding site is blocked by ATA.

Virus infection usually causes host cell apoptosis, and AgNPs could reduce the apoptosis caused by H1N1 virus infection by producing ROS. Researchers synthesized AgNPs loaded with zanamivir, a compound that inhibits caspase-3-mediated cell apoptosis by generating ROS, and this ROS-mediated cell apoptosis downregulation is related to the p38 and p53 signaling pathways.[48] In our ATA nanocomposites, both AgNPs and TiO_2 nanoparticles can induce ROS

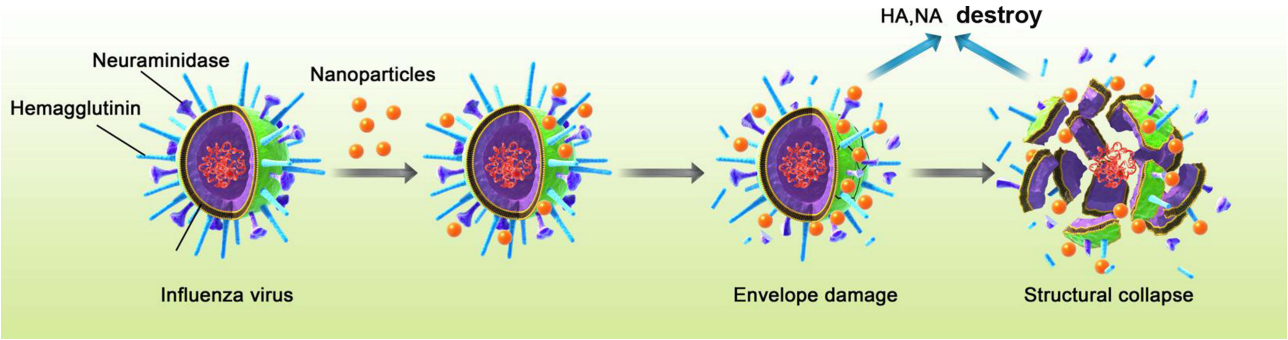

Figure 5 Schematic diagram of ATA anti-influenza virus mechanism. The H1N1 influenza virus is an enveloped, negative-strand RNA virus with a segmented genome. Its virion is typically 80 to 120 nm in diameter. The H1N1 influenza virus possesses two surface glycoproteins: HA and NA, which are determinants of virus infectivity, transmissibility, pathogenicity, host specificity, and major antigenicity. HA triggers erythrocyte aggregation by binding to sialic acid and facilitates viral attachment to infected cells, thereby enabling endocytosis. NA is essential for virus budding, cleaving sialic acid receptors and promoting virus spread to neighboring cells. Our results showed that ATA exerts its antiviral effect mainly by interfering with viral surface receptors rather than viral nucleic acids. The process of virus inactivation is mainly due to the damage of ATA to the envelope proteins of the influenza virus HA and NA, reducing the activity and expression of HA and NA proteins, damaging the virus structure, thereby killing the virus or preventing the virus from infecting the host cells. (ATA: Ag/TiO_2; HA: hemagglutinin; NA: neuraminidase).

production, which may be related to the molecular mechanism of the ATA-mediated anti-influenza virus. At the same time, excessive ROS production is also cytotoxic to mammalian cells, which may cause DNA damage and enhance proinflammatory responses in cells. Despite the wide application of AgNPs and ATA nanocomposites in disinfection, there are still potential hazards and limitations due to the toxicity and environmental impact of AgNPs. ATA exerts antiviral effects in a dose - and time-dependent manner, and similarly, the potential risk of side effects increases with increasing concentration and exposure time. In this study, we initially discussed the killing effect of ATA on the H1N1 influenza virus, and our team is also conducting the killing effect of ATA on a variety of bacteria and dust mites and conducted an in-depth study on the toxic effect of ATA.

Conclusion

In this study, we have observed a significant inactivation of influenza H1N1 viruses as a result of their exposure to ATA nanoparticles. The data suggest that the inactivation of the influenza H1N1 viruses depends on the concentration level and exposure time. The viral inactivation process is primarily attributed to the damage to the viral surface proteins of HA and NA, including the damage to the viral surface structure, protein activity and expression. Under the similar effect of H1N1 influenza virus inactivation, the concentration of AgNPs contained in the ATA nanocomposite prepared in this study was significantly lower than that of AgNPs, which greatly reduced the amount of AgNPs and reduced the side effects. The results of the present study suggest that ATA may be a good virucidal candidate against the influenza virus.

Viruses, bacteria and other microorganisms can be transmitted to the host through the air, and the large accumulation of dust in heating, air conditioning and other equipment creates favorable conditions for the spread of microorganisms. Although modern HEPA nets have been used to limit the spread of viruses and bacteria, they are still unable to effectively inactivate various microorganisms attached to them, posing a significant potential risk to human health.[20] By attaching AgNPs to nanoporous membranes, multi-layer filters with different porosity can be designed. The antimicrobial properties of AgNPs combined with nanopores generated by spinning nanofibers not only provide excellent air purification performance but also increase the microbial killing effect.[49] Researchers have verified the killing effect of air filters with AgNP-coated silica particles on aerosol bacteriophage MS2 and IFVA under continuous airflow conditions. MS2 and IFVA viruses directly interact with Ag nanoparticles of the filters to inactivate the viruses.[50] Attaching ATA to the HEPA network and using it in the air purifier can also effectively prevent the potential toxicity of silver particles in the environment when they play the role of resisting many kinds of microorganisms. It may be an important strategy to prevent influenza virus infection in the early stage of virus transmission.

Abbreviations

HA, hemagglutinin; NA, neuraminidase; AgNPs, silver nanoparticles; CPE, cytopathic effect; TiO_2, titanium dioxide; ROS, reactive oxygen species; HEPA, high-efficiency particulate air; ATA, Ag/TiO_2; UV-vis, ultraviolet-visible; XRD, X-ray diffraction; SEM, scanning electron microscopy; HR-TEM, high-resolution transmission electron microscopy; EDX, energy dispersive X-ray spectroscopy; MDCK, Madin-Darby canine kidney; DMEM, Dulbecco's modified Eagle's medium; $TCID_{50}$, 50% tissue culture infectious dose; HI, hemagglutination inhibition; WB, western blotting; RT-PCR, reverse transcription-polymerase chain reaction; PB2, polymerase basic protein 2; PB1, polymerase basic protein 1; PA, polymerase acidic protein; NP, nucleoprotein; M, matrix protein; NS, non-structural protein.

Acknowledgments

This study was supported by grants from the National Natural Science Foundation of China (No.82341060, 82073950, 22106108, 82204883), Science and Technology Planning Project of Guangdong Province (No.2023A1515012245, 2022B1515120055, 2024A1515011412), Shenzhen Science and Technology Program (No. SGDX20201103095609027, JCYJ20200109143435556, JCYJ20220818102005011), Sponsored by Open Project of State Key Laboratory of Respiratory Disease (No.SKLRD-Z-202204, SKLRD-OP-202410), Supported by Medical-Engineering Interdisciplinary Research Foundation of ShenZhen University (No.2023YG029).

Disclosure

The author(s) report no conflicts of interest in this work.

References

1. Tanner AR, Dorey RB, Brendish NJ, et al. Influenza vaccination: protecting the most vulnerable. *Eur Respir Rev*. 2021;30(159):200258. doi:10.1183/16000617.0258-2020
2. Gertz A, Rader B, Sewalk K, et al. Decreased seasonal influenza rates detected in a crowdsourced influenza-like illness surveillance system during the COVID-19 pandemic: prospective cohort study. *JMIR Public Health Surveill*. 2023;9(1):e40216. doi:10.2196/40216
3. Shope RE. Swine influenza: III. Filtration experiments and etiology. *J Exp Med*. 1931;54(3):373–385. doi:10.1084/jem.54.3.373
4. Mazel-Sanchez B, Iwaszkiewicz J, Bonifacio P, et al. Influenza A viruses balance ER stress with host protein synthesis shut off. *Proc Natl Acad Sci*. 2021;118(36):e2024681118. doi:10.1073/pnas.2024681118
5. Hirst GK. The agglutination of red cells by allantoic fluid of chick embryos infected with influenza virus. *Science*. 1941;94(2427):22–23. doi:10.1126/science.94.2427.22
6. Herrler G, Rott R, Klenk HD, et al. The receptor-destroying enzyme of influenza C virus is neuraminate-O-acetylesterase. *EMBO J*. 1985;4(6):1503–1506. doi:10.1002/j.1460-2075.1985.tb03809.x
7. Batool S, Chokkakula S, Song MS. Influenza treatment: limitations of antiviral therapy and advantages of drug combination therapy. *Microorganisms*. 2023;11(1):183. doi:10.3390/microorganisms11010183
8. Agor JK, Özaltın OY. Models for predicting the evolution of influenza to inform vaccine strain selection. *Hum Vaccines Immunother*. 2018;14(3):678–683. doi:10.1080/21645515.2017.1423152
9. Ahire SA, Bachhav AA, Pawar TB, et al. The augmentation of nanotechnology era: a concise review on fundamental concepts of nanotechnology and applications in material science and technology. *Res Chem*. 2022;4:100633. doi:10.1016/j.rechem.2022.100633
10. Liz-Marzán LM, Nel AE, Brinker CJ, et al. What do we mean when we say nanomedicine?. *ACS Nano*. 2022;16(9):13257–13259. doi:10.1021/acsnano.2c08675
11. Hegde M, Pai P, Shetty MG, et al. Gold nanoparticle based biosensors for rapid pathogen detection: a review. *Environ Nanotechnol Monit Manage*. 2022;18:100756. doi:10.1016/j.enmm.2022.100756
12. Valenzuela-Amaro HM, Aguayo-Acosta A, Meléndez-Sánchez ER, et al. Emerging applications of nanobiosensors in pathogen detection in water and food. *Biosensors*. 2023;13(10):922. doi:10.3390/bios13100922
13. Sánchez-López E, Gomes D, Esteruelas G, et al. Metal-based nanoparticles as antimicrobial agents: an overview. *Nanomaterials*. 2020;10(2):292. doi:10.3390/nano10020292
14. Bankier C, Matharu RK, Cheong YK, et al. Synergistic antibacterial effects of metallic nanoparticle combinations. *Sci Rep*. 2019;9(1):16074. doi:10.1038/s41598-019-52473-2
15. Bruna T, Maldonado-Bravo F, Jara P, et al. Silver nanoparticles and their antibacterial applications. *Int J Mol Sci*. 2021;22(13):7202. doi:10.3390/ijms22137202
16. Maduray K, Parboosing R. Metal nanoparticles: a promising treatment for viral and arboviral infections. *Biol Trace Elem Res*. 2021;199(8):3159–3176. doi:10.1007/s12011-020-02414-2
17. Xiang D, Zheng Y, Duan W, et al. Inhibition of A/Human/Hubei/3/2005 (H3N2) influenza virus infection by silver nanoparticles in vitro and in vivo. *Int j Nanomed*;2013. 4103–4114. doi:10.2147/IJN.S53622
18. Naumenko K, Zahorodnia S, Pop CV, et al. Antiviral activity of silver nanoparticles against the influenza A virus. *J Virus Erad*. 2023;9(2):100330. doi:10.1016/j.jve.2023.100330

19. Galdiero S, Falanga A, Vitiello M, et al. Silver nanoparticles as potential antiviral agents. *Molecules*. 2011;16(10):8894–8918. doi:10.3390/molecules16108894
20. Luceri A, Francese R, Lembo D, et al. Silver nanoparticles: review of antiviral properties, mechanism of action and applications. *Microorganisms*. 2023;11(3):629. doi:10.3390/microorganisms11030629
21. Rodríguez-González V, Obregón S, Patrón-Soberano OA, et al. An approach to the photocatalytic mechanism in the TiO2-nanomaterials microorganism interface for the control of infectious processes. *Appl Catal B*. 2020;270:118853. doi:10.1016/j.apcatb.2020.118853
22. Yamaguchi M, Abe H, Ma T, et al. Bactericidal activity of TiO2 nanotube thin films on Si by photocatalytic generation of active oxygen species. *Langmuir*. 2020;36(42):12668–12677. doi:10.1021/acs.langmuir.0c02225
23. De Pasquale I, Porto CL, Dell'Edera M, et al. TiO2-based nanomaterials assisted photocatalytic treatment for virus inactivation: perspectives and applications. *Curr Opin Chem Eng*. 2021;34:100716. doi:10.1016/j.coche.2021.100716
24. Zhang C, Li Y, Shuai D, et al. Progress and challenges in photocatalytic disinfection of waterborne viruses: a review to fill current knowledge gaps. *Chem Eng J*. 2019;355:399–415. doi:10.1016/j.cej.2018.08.158
25. Shiraki K, Yamada H, Yoshida Y, et al. Improved photocatalytic air cleaner with decomposition of aldehyde and aerosol-associated influenza virus infectivity in indoor air. *Aerosol Air Qual Res*. 2017;17(11):2901–2912. doi:10.4209/aaqr.2017.06.0220
26. Jeon JP, Kweon DH, Jang BJ, et al. Enhancing the photocatalytic activity of TiO2 catalystsTiO 2 catalysts. *Adv Sustainable Syst*. 2020;4(12):2000197. doi:10.1002/adsu.202000197
27. Chakhtouna H, Benzeid H, Zari N, et al. Recent progress on Ag/TiO 2 photocatalysts: photocatalytic and bactericidal behaviors. *Environ Sci Pollut Res* 2021;28(33):44638–44666. doi:10.1007/s11356-021-14996-y
28. Moongraksathum B, Chien MY, Chen YW. Antiviral and antibacterial effects of silver-doped TiO2 prepared by the peroxo sol-gel method. *J of NanoscI Nanotech*. 2019;19(11):7356–7362. doi:10.1166/jnn.2019.16615
29. Chen S, Guo Y, Zhong H, et al. Synergistic antibacterial mechanism and coating application of copper/titanium dioxide nanoparticles. *Chem Eng J*. 2014;256:238–246. doi:10.1016/j.cej.2014.07.006
30. Chen S, Guo Y, Chen S, et al. Facile preparation and synergistic antibacterial effect of three-component Cu/TiO 2/CS nanoparticles. *J Mater Chem*. 2012;22(18):9092–9099. doi:10.1039/c2jm00063f
31. Lei C, Yang J, Hu J, et al. On the calculation of TCID 50 for quantitation of virus infectivity. *Virologica Sin*. 2021;36(1):141–144. doi:10.1007/s12250-020-00230-5
32. Reed LJ, Muench H. A simple method of estimating fifty percent endpoints. *American Journal of Epidemiology*. 1938;27(3):493–497. doi:10.1093/oxfordjournals.aje.a118408
33. World Health Organization. WHO manual on animal influenza diagnosis and surveillance[R]. *World Health Organization*. 2002;2002.
34. Jiang Z, Ouyang Q, Peng B, et al. Ag size-dependent visible-light-responsive photoactivity of Ag–TiO $_2$ nanostructure based on surface plasmon resonance. *J Mater Chem A*. 2014;2(46):19861–19866. doi:10.1039/C4TA03831B
35. Imai K, Ogawa H, Bui VN, et al. Inactivation of high and low pathogenic avian influenza virus H5 subtypes by copper ions incorporated in zeolite-textile materials. *Antiviral Res*. 2012;93(2):225–233. doi:10.1016/j.antiviral.2011.11.017
36. Haggag EG, Elshamy AM, Rabeh MA, et al. Antiviral potential of green synthesized silver nanoparticles of Lampranthus coccineus and malephora lutea. *Int j Nanomed*. 2019;Volume 14:6217–6229. doi:10.2147/IJN.S214171
37. Horie M, Ogawa H, Yoshida Y, et al. Inactivation and morphological changes of avian influenza virus by copper ions. *Arch Virol*. 2008;153(8):1467–1472. doi:10.1007/s00705-008-0154-2
38. Sieben C, Sezgin E, Eggeling C, et al. Influenza A viruses use multivalent sialic acid clusters for cell binding and receptor activation. *PLoS Pathogens*. 2020;16(7):e1008656. doi:10.1371/journal.ppat.1008656
39. Yamada K, Ogawa H, Hara A, et al. Mechanism of the antiviral effect of hydroxytyrosol on influenza virus appears to involve morphological change of the virus. *Antiviral Res*. 2009;83(1):35–44. doi:10.1016/j.antiviral.2009.03.002
40. Liu L, Chen G, Huang S, et al. Receptor binding properties of neuraminidase for influenza A virus: an overview of recent research advances. *Virulence*. 2023;14(1):2235459. doi:10.1080/21505594.2023.2235459
41. Gubareva L, Mohan T. Antivirals targeting the neuraminidase. *Cold Spring Harb Perspect Med*. 2022;12(1):a038455. doi:10.1101/cshperspect.a038455
42. Nayak DP, Balogun RA, Yamada H, et al. Influenza virus morphogenesis and budding. *Virus Res*. 2009;143(2):147–161. doi:10.1016/j.virusres.2009.05.010
43. Huang T, Li X, Maier M, et al. Using inorganic nanoparticles to fight fungal infections in the antimicrobial resistant era. *Acta Biomater*. 2023;158:56–79. doi:10.1016/j.actbio.2023.01.019
44. Arshad F, Naikoo GA, Hassan IU, et al. Bioinspired and green synthesis of silver nanoparticles for medical applications: a green perspective. *Appl Biochem Biotechnol* 2024;196(6):3636–3669. doi:10.1007/s12010-023-04719-z
45. Tomaszewska E, Ranoszek-Soliwoda K, Bednarczyk K, et al. Anti-HSV activity of metallic nanoparticles functionalized with sulfonates vs. polyphenols. *Int J Mol Sci*. 2022;23(21):13104. doi:10.3390/ijms232113104
46. Behzad F, Kalyani FN, Samadi A, et al. A promising treatment for HIV-1 using biosynthesis of metal nanoparticles. *J Ind Eng Chem*. 2022;115:20–25. doi:10.1016/j.jiec.2022.07.052
47. Bullough PA, Hughson FM, Skehel JJ, et al. Structure of influenza haemagglutinin at the pH of membrane fusion. *Nature*. 1994;371(6492):37–43. doi:10.1038/371037a0
48. Lin Z, Li Y, Guo M, et al. The inhibition of H1N1 influenza virus-induced apoptosis by silver nanoparticles functionalized with zanamivir. *RSC Adv*. 2017;7(2):742–750. doi:10.1039/C6RA25010F
49. Ju Y, Han T, Yin J, et al. Bumpy structured nanofibrous membrane as a highly efficient air filter with antibacterial and antiviral property. *Science of the Total Environment*. 2021;777:145768. doi:10.1016/j.scitotenv.2021.145768
50. Joe YH, Woo K, Hwang J. Fabrication of an anti-viral air filter with SiO2–Ag nanoparticles and performance evaluation in a continuous airflow condition. *J Hazard Mater*. 2014;280:356–363. doi:10.1016/j.jhazmat.2014.08.013